Available online at www.sciencedirect.com
SCIENCE DIRECT®
Journal of Non-Crystalline Solids 351 (2005) 1512–1521
JOURNAL OF NON-CRYSTALLINE SOLIDS
www.elsevier.com/locate/jnoncrysol

Nucleation time lag at nano-sizes

V.A. Shneidman *, E.V. Goldstein

Department of Physics, New Jersey Institute of Technology, Newark, NJ 07102, USA

Received 6 December 2004

Abstract

A rapidly convergent exact expression for the time lag (also, 'induction time') of transient nucleation obtained by Shneidman and Weinberg [J. Chem. Phys. 97 (1992) 3629] is used to evaluate the lag for clusters with up to 10^8 monomers. Asymptotic approximations to the exact expression are further advanced to provide explicit elementary expressions for the time lag in the Turnbull–Fisher (TF) nucleation model in various domains of parameters. The difference between the TF time lag and the one of Zeldovich–Frenkel nucleation equation is examined in detail. Transient nucleation flux and the number of nuclei are also discussed, and analytical results appear to be in very good agreement with numerical solutions of the TF equations at large sizes, as reported by Granasy and James [J. Chem. Phys. 113 (2000) 9810].

PACS: 64.60.Qb

1. Introduction and background

Among the vast scope of scientific interests of Mike Weinberg an important place was occupied by the topic of time-dependent nucleation. He had an unmatched understanding of all aspects of this problem, from experimental implications to very refined analytics, always with a strong emphasis on the simplicity of the final results. Examples include corrections to Kolmogorov–Avrami expression, nucleation and crystallization upon rapid heating, evaluation of the nucleation barrier and crystal-to-melt interfacial tension from transient nucleation data, etc. The problem of time lag ('induction time'), which attracted Mike's attention in early 90s, was of special status in the nucleation theory and its solution allowed to bring together several previously unrelated directions.

In the crystallization context the standard classical-type nucleation picture is due to Turnbull and Fisher (TF) [1]. Theoretical studies related to the time-dependent aspects of the problem are driven by experiments in silicate glasses [2–6], amorphous thin films [7,8], nucleation and growth of quantum dots [9], etc. Numerical solutions of the TF equations are also available [8,10,11]. Other models, such as the 'Zeldovich–Frenkel' (ZF) or the Becker–Döring (BD) equations are also discussed for condensed systems, but more typically those models are associated with condensation of dilute vapors.

In Ref. [12] it was shown that exact expressions for the time lag can be cast in terms of rapidly convergent sums. In the limit of a high nucleation barrier in case of the TF model the exact sums were also evaluated asymptotically. Here the barrier- and size-dependences could be separated, and the latter was expressed in terms of growth/decay integrals, $\int dR/v(R)$, R being the radius of a nucleus and $v(R)$ the 'deterministic growth rate' (see Section 1.2 for a more

* Corresponding author. Tel.: +1 973 596 3555; fax: +1 973 596 5794.
E-mail address: vitaly@oak.njit.edu (V.A. Shneidman).

0022-3093/$ - see front matter © 2005 Elsevier B.V. All rights reserved.
doi:10.1016/j.jnoncrysol.2005.03.039

precise definition). The general expression was similar to the one following from the matched asymptotic solution of the ZF and BD equations [13,14], but with a different $v(R)$ appropriate for the TF model [15]. Also, in contrast to the ZF case where due to a very simple $v(R)$ the integrals could be expressed in elementary functions, the general TF expression could not be further simplified. From a practical point having to evaluate an integral can represent a serious obstacle in application of the results, and, the very fact that solutions to the discrete nucleation equations exist remained mostly unknown. The matched asymptotic solution of the ZF equations had more applications [4,8,11], but since the standard model is the TF one it could be extremely important to quantify the differences.

For the time lag, the difference between the TF and the ZF predictions at the critical size can be evaluated [12], but is typically small [16,17] and anyway is mostly of academic interest. The situation is less simple in the growth region which is more relevant to experimental measurements.

As far as one considers modest values of the size R in the growth regime (say, 2–3R_*), the solution to the ZF model [14] can provide a reasonable starting approximation [12,17]. Indeed, independent numerical studies of the full transient problem [8] confirmed the accuracy of elementary expressions. At the same time if one proceeds to the region of larger R, even minor differences in the growth rates accumulate in the growth time, and the difference in the transient solutions for the ZF and TF models becomes noticeable. As a temporal remedy one could still use the ZF solution, adjusting only the term associated with growth of large particles to its TF value [18]. This allowed to describe transient solutions for $R \lesssim 5R_*$. The possibility to check large sizes at the time was limited by the amount of equations which could be solved (and which should exceed $(R/R_*)^3 n_*$ with n_*, the critical number, being of the order of several tens). With rapid advance in computer power, however, Granasy and James [11] were able to solve up to 200 000 equations which allowed them to consider sizes up to 20 R_*. At such sizes they observed minor deviations between their data and the interpolating expression [18].

The intent of the present study is to clarify the structure of the time lag in the TF model at very large R when the difference from the ZF case becomes appreciable. From an analytical point having an additional large parameter simplifies the treatment, and indeed often leads to elementary expressions. Exact data are used to monitor the accuracy of the approximations. Transient curves are also evaluated. For the TF model the difference with the data by Granasy and James disappears at least within the reported limits of accuracy.

1.1. Main parameters of the nucleation equation

The general master equation of the nucleation problem has the form

$$\mathrm{d}f_n/\mathrm{d}t = j_n - j_{n+1}, \quad j_n = \beta_{n-1} f_{n-1} - \alpha_n f_n. \tag{1}$$

Here f_n is the density of nuclei which contain n monomers, and j_n is the flux in the n-space. The gain and loss coefficients are connected through the minimal work, $W(n)$, which is required to form a nucleus via the detailed balance condition

$$\alpha_n = \beta_{n-1} \exp\{[W(n) - W(n-1)]/T\}. \tag{2}$$

(Boltzmann constant is taken as 1.) The (quasi)equilibrium distribution, which would correspond to a zero flux, is given by $f_n^{\mathrm{eq}} = f_1 \exp\{-W(n)/T\}$. Maximum of the work W is achieved at the critical number $n = n_*$. The boundary conditions are taken as $f(n_{\min}) = f_n^{\mathrm{eq}}(n_{\min})$ at some small $n_{\min} \ll n_*$, while $f_n \to 0$ for $n \to \infty$.

In the Turnbull–Fisher model one has [10]

$$\beta_n \propto n^{2/3} \exp\{[W(n) - W(n+1)]/2T\}. \tag{3}$$

Within the classical approach the work W is taken as

$$W(r) = W_*(3r^2 - 2r^3), \quad r = (n/n_*)^{1/3} \tag{4}$$

with W_* corresponding to the barrier to nucleation and r being the dimensionless 'radius'. It is assumed that W_* is large compared to T and

$$\epsilon = \left(-\frac{1}{T} \frac{\mathrm{d}^2 W}{\mathrm{d}r^2}\bigg|_* \right)^{-1/2} = \left(\frac{6W_*}{T} \right)^{-1/2} \ll 1, \tag{5}$$

determines the main small parameter of the nucleation problem. [To avoid confusion with notations, note that in previous publications we used ϵ which differs by a constant]. There is also another small parameter, namely the inverse of the critical number n_*^{-1}. For simplicity of the discussion, we assume that a combination of the two

$$a = 2\frac{W_*}{Tn_*} = \frac{1}{3n_*\epsilon^2}, \tag{6}$$

remains finite for $\epsilon \to 0$ or $n_* \to \infty$, but otherwise a can be large or small compared to unity. Note that finite difference in Eq. (1) can be replaced by derivatives (which would make it the Zeldovich–Frenkel equation) when $a \to 0$, so the latter plays the role of a 'discreteness parameter' [12].

1.2. Growth rate

The deterministic growth rate, $\dot{n}$, is introduced from the condition that for a smooth function f_n in Eq. (1), the flux j_n should approach the drift flux, $\dot{n} f_n$. Further, this rate is also 'macroscopic', in the sense that changes in n by ± 1 should result in only minor effects, and finite

differences of 'smooth' functions are replaced by derivatives. In terms of r one has

$$v(r) = \dot{n}/(3n_*^{1/3}n^{2/3}). \tag{7}$$

The growth rate changes sign at the critical size, and the main time scale [19] can be defined as

$$\tau^{-1} = \left.\frac{\mathrm{d}v(r)}{\mathrm{d}r}\right|_* \simeq \beta_*/(9n_*^2\epsilon^2). \tag{8}$$

The ZF growth rate is given by

$$\tau v^{\mathrm{ZF}}(r) = 1 - 1/r \equiv \zeta(r), \tag{9}$$

and the dimensionless function ζ(r) will play an important role in further discussion. Alternatively, the TF rate is given by Kelton and Greer [15]

$$v(r) = \frac{2}{a\tau}\sinh[a\zeta/2]. \tag{10}$$

According to Zeldovich [19] the same time scale τ which enters into the growth rate also determines the pre-exponential of the steady-state nucleation rate

$$j_{\mathrm{s}} \simeq \frac{3\epsilon n_*}{\tau\sqrt{2\pi}} f_1 \exp\left\{-\frac{W_*}{T}\right\}. \tag{11}$$

The above expression is asymptotic, valid for $\epsilon \ll 1$ and $\epsilon n_* \gg 1$. Similar requirements will be assumed in the time-dependent case discussed below. An exact steady-state flux $j_{\mathrm{s}}^{\mathrm{e}}$ (with very close numerical values) is also available due to Farkas [20] and is given in Appendix A.

1.3. The transient solution

The full transient problem can be treated asymptotically, but not exactly. The matched asymptotic: solution of the nucleation equation [13,14] gives the flux

$$j(r,t)/j_{\mathrm{s}} = \exp\{-\exp[(t_i(r) - t)/\tau]\} \tag{12}$$

with 'incubation time'

$$t_i(r) = t_{\mathrm{dec}}(1-\epsilon, 0) + t_{\mathrm{gr}}(1+\epsilon, r). \tag{13}$$

Here t_{dec} and t_{gr} are positive decay and growth times, respectively with indicated initial and finite sizes (i.e. the integrals $\int \mathrm{d}r/v(r)$ with indicated integration limits). As a reference, we will be using the elementary $t_i(r)$ for the ZF equation [14]

$$t_i^{\mathrm{ZF}}(r,\epsilon) = \tau\left\{r - 2 + \ln(r-1) + \ln\left(\frac{1}{\epsilon^2}\right)\right\}. \tag{14}$$

Separation of the barrier-dependent term is typical, but otherwise the r-dependence is specific for the model considered. Strictly speaking, Eq. (12) was derived for the ZF and the BD cases [13,14], and the TF model, which has less smooth coefficients β_n could require a more careful analysis. At the moment, however, there seems to be no reasons to disbelieve this equation, in particular because it predicts a time-lag (see next section) which is consistent with the exact expression [12]. Thus, below we focus on the more accurate evaluation of t_i, appropriate for the TF case, otherwise relying on Eq. (12) for the transient shape.

In case $n_{\min}$, which locates the lower boundary, makes a noticeable fraction of n_*, the incubation time is reduced by the corresponding decay time

$$t_i(r, r_{\min}) = t_i(r) - t_{\mathrm{dec}}(r_{\min}) \tag{15}$$

with $r_{\min} = (n_{\min}/n_*)^{1/3} < 1$. In the ZF case one has

$$t_{\mathrm{dec}}^{\mathrm{ZF}}(r_{\min})/\tau = -\ln(1 - r_{\min}) - r_{\min} \tag{16}$$

but for discrete models t_{dec} cannot be evaluated in elementary functions and approximations will be discussed later in the paper. Detailed numeric studies of the effects of the lower boundary for the Becker–Döring equation have been performed by Shizgal and Barret [21] in terms of the time-lag, and results are well reproduced by Eq. (15) [12]. In what follows, we will refine the general expression for t_{dec}, and propose some elementary approximations for the TF model.

1.4. The time lag

The time-lag is defined as

$$t_{\mathrm{L}}(r) = \lim_{t\to\infty}\{t - \rho(r,t)/j_{\mathrm{s}}\}, \quad \rho(r,t) = \int_0^t j(r,t)\,\mathrm{d}t. \tag{17}$$

Eq. (12) predicts the following relations for the number of nuclei [14]

$$\rho(r,t) = \tau j_{\mathrm{s}} E_1\left[\exp\left(-\frac{t - t_i(r)}{\tau}\right)\right] \tag{18}$$

(with E_1 being the first exponential integral [22]) and the time lag is given by Shneidman [14]

$$t_{\mathrm{L}}(r) = t_i(r) + \gamma\tau, \quad \gamma = 0.5772\ldots \tag{19}$$

with γ being Euler constant. The above relations are asymptotic, valid for a high barrier and the size r in the growth region, (i.e. $r - 1 \gg \epsilon$). An exact time lag $t_{\mathrm{L}}^{\mathrm{e}}$ of Ref. [12] is given in Appendix A.

1.5. Experimental meaning of parameters

Since, unlike j_{s} the transient flux $j(r,t)$ depends on reduced size r, experimental meaning of this parameter should be clarified. If R_* is the radius of the critical nucleus, in one-step annealing experiments $R = rR_*$ corresponds to the lowest detectable size, usually much larger than R_*. Similarly, the distribution of nuclei over sizes, as observed, e.g., in the TEM studies of amorphous thin films [7,8] corresponds to $R_*^{-1}j(r,t)/v(r)$.

In two-step annealing R is the critical size at the higher (development) temperature if heating between the two stages is fast. There has been some confusion

in literature regarding to what happens for a finite heating rate [23]. Most likely, the above transient expressions will remain valid in that case as well, but R will have a meaning of the 'survival size' [24], i.e. the smallest size which will grow after heating is completed.

2. Analytical and computational methods

2.1. General

It is convenient to express the incubation time as a correction to the elementary expression for the ZF equation, t_i^{ZF} in Eqs. (14)–(16):

$$t_i(r,\epsilon,a) = t_i^{\mathrm{ZF}}(r,\epsilon) + \delta t_i(a,r), \tag{20}$$

δt_i, which is independent of the barrier, is given by

$$\frac{1}{\tau}\delta t_i(a,r) = \mathscr{F}[\zeta(r)] + \mathscr{F}[\zeta(r_{\min})] \tag{21}$$

with

$$\mathscr{F}[\zeta] = \int_0^{\zeta} \frac{\mathrm{d}\zeta}{(1-\zeta)^2}\left(\frac{1}{\tau v} - \frac{1}{\zeta}\right). \tag{22}$$

The same correction can be used for the time lag, due to Eq. (19). Note that Eq. (13) is singular for $\epsilon \to 0$ since both t_{gr} and t_{dec} diverge near $r = 1$. However, the ZF approximation to the growth rate, Eq. (10), takes care of this singularity and the integrand in Eq. (21) remain finite near the critical size, which corresponds to $\zeta = 0$.

For $r \gg 1$ one can keep only the divergent parts of the integral as $\zeta \to 1$, which gives

$$\frac{1}{\tau}\delta t_i(a,r) = r[F(a) - 1] + \ln r[G(a) - 1] - 2 + D(a). \tag{23}$$

Here $D(a)$ is a constant which is defined to be zero in the ZF limit $a \to 0$, while F and G follow from the expansion of the growth rate at large r:

$$F(a) = \frac{a}{2\sinh(a/2)}, \quad G(a)/F(a) = (a/2)\coth(a/2). \tag{24}$$

(Similar terms appear when describing the transient nucleation corrections to the Kohnogorov–Avrami expression for the crystallized volume fraction [25].)

The value of the constant $D(a)$ is given by an integral

$$D(a) = \int_0^{\infty} \mathrm{d}r\left\{\frac{1}{|\zeta(r)|}\left(\frac{\zeta(r)}{\tau v(r)} - 1\right) - (F(a) - 1) - \frac{G(a) - 1}{r + 1}\right\}, \tag{25}$$

which converges near $r = 1$, as well as for $r \to \infty$, albeit not too fast.

2.2. Expansion in Bernoulli numbers: moderate discreteness effects

For small values of $|a\zeta|$ the inverse growth rates can be expanded around the ZF expression as

$$\frac{1}{\tau v[\zeta]} = \frac{1}{\zeta} + \sum_{k=2}^{\infty} a^k b_k \zeta^{k-1}, \quad |a\zeta| < 2\pi. \tag{26}$$

The coefficients b_k are expressed through Bernoulli numbers, B_k^{22}, as

$$b_k = -B_k(1 - 2^{1-k})/k!. \tag{27}$$

For reference, $b_2 = -1/24$, $b_4 \approx 0.001215$, $b_6 \approx = -3.2 \times 10^{-5}$, and all b_k with odd k are zero.

The correction to the ZF time-lag can be obtained using the term-by-term integration. The result for the $(k+1)$st term in the sum ($k \geqslant 4$) will contain a regular, polynomial part

$$p_{k+1}(\zeta) = \int_0^{\zeta} \frac{z^k - 1 + k(1-z)}{(1-z)^2}\,\mathrm{d}z = \sum_{m=1}^{k-1} \frac{m}{k-m}\zeta^{k-m}, \tag{28}$$

and two terms which diverge as $\zeta \to 1$, respectively, as $1/(1-\zeta)$ and (for $k > 1$) as $\ln(1-\zeta)$. Summation of the diverging terms can be performed in all orders in a, resulting in

$$\mathscr{F}[\zeta] \simeq \frac{\zeta}{1-\zeta}(F(a) - 1) + (G(a) - 1)\ln\frac{1}{1-\zeta} + \sum_{k=4}^{\infty} a^k b_k p_k(\zeta) \tag{29}$$

with $F(a)$ and $G(a)$ given in Eqs. (24). This gives the size-dependence of the incubation time at arbitrary (not necessarily large) size $r > 1$. Note the absence of polynomial corrections in the lower orders in a, and the first of those contribution is $a^4 b_4 p_4(\zeta) \simeq (a/5.36)^4[2\zeta + \zeta^2/2]$. In the growth region with $0 < \zeta(r) < 1$ such corrections are exceptionally small (in practice, negligible) at $a \lesssim 1$, and deviation from the ZF size-dependence is mostly determined by the first two terms in Eq. (29). At the same time, when evaluating the decay integral the expansion in Bernoulli numbers is applicable only for an 'elevated bondary' (see below) since otherwise ζ has large negative values, and the condition in Eq. (26) can be violated. This will not change the size-dependence but will affect the constant D in Eq. (23) and will be discussed later in the paper.

2.3. Strong discreteness effects, $a \gg 1$

Here it is more convenient to start with Eq. (13) since correction to the ZF expression is not small anymore. The decay part of t_i can be expanded in terms of $1/a$

$$t_{\rm dec}(1-\epsilon) = \int_{a\epsilon/2}^{\infty} \frac{{\rm d}z}{(1+2z/a)^2 \sinh(z)} = -\ln\left|\tanh\frac{a\epsilon}{4}\right| - \frac{\pi^2}{a} + {\rm O}(1/a^2). \quad (30)$$

Evaluation of the growth integral in $t_{\rm gr}(1+\epsilon, r)$ involves more elaborate asymptotic analysis. The integration region is divided into two domains, between $1+\epsilon$ and some r_0 which satisfies a condition $1/a \ll r_0 - 1 \ll 1$, and between r_0 and $r \gg 1$. In the first region a linearization of the argument of $\sinh[a/2\cdot(1-1/r)]$ is possible with a resulting explicit evaluation of the integral. In the second region, $r \geqslant r_0$, one can use the exponential approximation for the $\sinh(z)$ at large arguments which, again, allows for an explicit evaluation of the integral in terms of the exponential integral E_i. For large values of a matching of the two regions is asymptotically smooth, leading to a result which is independent of r_0. Adding Eq. (30) gives the incubation time

$$t_i^{\rm TF}(r,a) = -2\ln\left|\tanh\frac{a\epsilon}{4}\right| + rF(a) - G(a)E_i\left(\frac{a}{2r}\right) - \frac{\pi^2}{a} + \cdots. \quad (31)$$

The functions $F(a)$ and $G(a)$ are re-introduced for consistency of notations, but strictly speaking, within the accuracy of the treatment they should be replaced by their large-a asymptotes.

If one further considers the limit of large sizes $r \gg a/2$ and expands the ln |tanh| function for $\epsilon \to 0$, one recovers the general form. Eq. (23), with the leading term in the $D(a)$ dependence given by

$$D(a) \simeq 2 + 2\ln(4/a), \quad a \gg 1. \quad (32)$$

The first neglected correction is π^2/a which is typically not a small number, and indeed this asymptotic approximation becomes accurate only for relatively large (and in practice, not too realistic) values of a. Alternative approximations will be discussed.

2.4. Interpolation for arbitrary a, and the limit $a \to 0$

One can approximate the TF growth rate as

$$\frac{1}{\tau v(r)} \simeq \frac{1}{\zeta(1+\zeta^2 b^2)}, \quad b = \frac{qa}{2\pi}. \quad (33)$$

At the moment, parameter q, which is close to 1, is kept flexible and will be treated as an adjustable parameter. With $q = \pi/\sqrt{6} \approx 1.28$, Eq. (33) corresponds to the [0/3] Padé approximation. Keeping only the leading terms, one obtains

$$D(a) \simeq a^2\ln(a)/24, \quad a \to 0. \quad (34)$$

This refines the earlier estimation [12] by including a constant. Although formally valid only for small $a \to 0$, the above asymptote remains acceptable for larger $a \lesssim 1$, reasonably describing the local shallow minimum at $a \approx 0.6$, and slightly less accurately, the change of sign near $a \approx 1$.

To interpolate for arbitrary a, we perform an explicit integration for a general q which gives

$$\mathscr{F}[b,\zeta] \approx -\frac{b^2\zeta}{(b^2+1)(1-\zeta)} + \frac{2b^3\tan^{-1}[b\zeta]}{(b^2+1)^2} - \frac{b^2(b^2-1)}{2(b^2+1)^2}\ln\frac{1+b^2\zeta^2}{(1-\zeta)^2}. \quad (35)$$

In principle, this function allows one to describe all sizes in the growth region, as well as the decay region with large negative ζ; the value of a can be arbitrary. A way to systematically improve the accuracy will be given in Appendix B.

For the constant $D(a)$ in the main Eq. (23) one has

$$D(a) \approx \frac{qb^2}{2(1+b^2)^2}\{4+4b^2-2b\pi+4b\tan^{-1}(b) - (b^2-1)\ln[b^2(b^2+1)]\}. \quad (36)$$

Non-rigorously, an extra factor q was included based on comparison with exact numerics. It turns out that $q \approx 1.3$. close to the Padé value, provides the best fit and Eq. (36) describes the entire domain of a.

2.5. D(a) from exact time lag

One can use the exact expressions for the time-lag and its connection with t_i. Eq. (19), and *define* $D^{\rm e}(a)$ as

$$D^{\rm e}(a) = \frac{t_{\rm L}^{\rm e}(r)}{\tau} - F(a)r - G(a)\ln r - \gamma + 2, \quad r \to \infty. \quad (37)$$

The difference in $D(a)$ and $D^{\rm e}(a)$ is obvious since $D(a)$ depends on fewer parameters, namely on the ratio $a = 2W_*/Tn_*$, while $t_{\rm L}^{\rm e}$ in $D^{\rm e}(a)$ depends on individual values of W_*/T and n_*. Nevertheless, if the asymptotic treatment is correct, i.e. if Eqs. (19) and (25) are valid, the values of D and $D^{\rm e}$ must be close, while $D^{\rm e}(a)$ should have a negligible dependence on W_* (or, on n_*) once a is fixed.

2.6. Computational

The major computational effort was associated with numerical evaluation of the time lag from the exact Eqs. (A.2)–(A.4). We avoided an artificial cut-off at some large N (replacing infinities in the summation limits) which would restrict sizes to $n < N$, and which would lead to an extremely long evaluations of the repeated sums for $n > 10^6$. Rather, a 'computer infinity' was achieved by adding terms until the sums no longer changed within prescribed accuracy. Due to rapid convergence, changing the accuracy level from 10^{-6} to 10^{-16}

resulted only in a modest increase of computational time and no significant change in the results. For $n \lesssim 10^5$ the *Mathematica* program could be used; a *C* program was written to cope with larger values.

Another computational issue is evaluation of the integral (25) to test the analytical approximations. The integral converges slowly, and requires a delicate compensation of potentially diverging terms. The *Mathematica* built-in numerical integration routine was used with added recursion option, to account for the increased accuracy requirements. A similar approach was used when evaluating the integrals in Eq. (13) which logarithmically diverge for $\epsilon \to 0$ and which (in the growth case) linearly diverge for $r \to \infty$.

3. Results

3.1. Exact evaluation of the lag and scaling of the results

As follows from previous discussion, the reduced time-lag

$$\tilde{t}_{\mathrm{L}}(a,r) = \frac{t_{\mathrm{L}}}{\tau} - \ln\left(\frac{6W_*}{T}\right) \tag{38}$$

is expected to be independent of the barrier, provided the latter is large. This is illustrated in Fig. 1 where for each a the corresponding barrier was doubled without any significant change in the location of points. Such data are also in good correspondence with the asymptotic Eqs. (13) and (19) which previously never were tested at such large sizes. Note, however, that for larger a a larger barrier is required to get the expected asymptotic behavior. Thus, from a practical point, the results for $a = 8$ are formal since nucleation at such high barriers is unrealistic. From a computational point, the most elaborate was verification of the ZF limit at small a. Here, with the critical size $n_* = 200$ values of n over 10^8 had to be considered for r close to 80, as in Fig. 1.

3.2. Analytic approximations

The general asymptotic expression for the incubation time, Eq. (13) (solid lines in Fig. 1) can be approximated at large sizes $r \gg 1$ as

$$\frac{1}{\tau}t_i(r,\epsilon,a) \simeq F(a)r + G(a)\ln r + \ln\frac{r-1}{r} + \ln\left(\frac{6W_*}{T}\right) - 2 + D(a). \tag{39}$$

The time lag differs by a constant, as in Eq. (19). The terms $F(a)$ and $G(a)$ are related, respectively, to size-independent growth rate of large nuclei and to curvature-dependent corrections [14] and are given in Eqs. (24). The logarithmic dependence on the barrier is due to contribution of near-critical sizes. The small term $D(a)$, on the other hand, is sensitive to the entire domain of sizes and, in a general case, requires a more elaborate asymptotic analysis. Strictly speaking, the term $\ln[(r-1)/r]$ is small for $r \gg 1$, but it ensures the proper ZF limit (small a) at arbitrary $r > 1$ which broadens the practical domain of applicability.

Note the asymptotic separation of the dependences on the main three dimensionless parameters, r, W_*/T, and a, with the barrier-dependence being the same as in the ZF case. All functions which enter Eq. (39) are elementary, although the dependence $D(a)$ at intermediate a is rather cumbersome, as in Eq. (36). Nevertheless, as long as D is a function of a *single* parameter, it can be easily interpolated. $D(a)$ is shown in Fig. 2 together with the large- and small-a asymptotes and the interpolating Eq. (36). Symbols were obtained from Eq. (37) with $r = 100$.

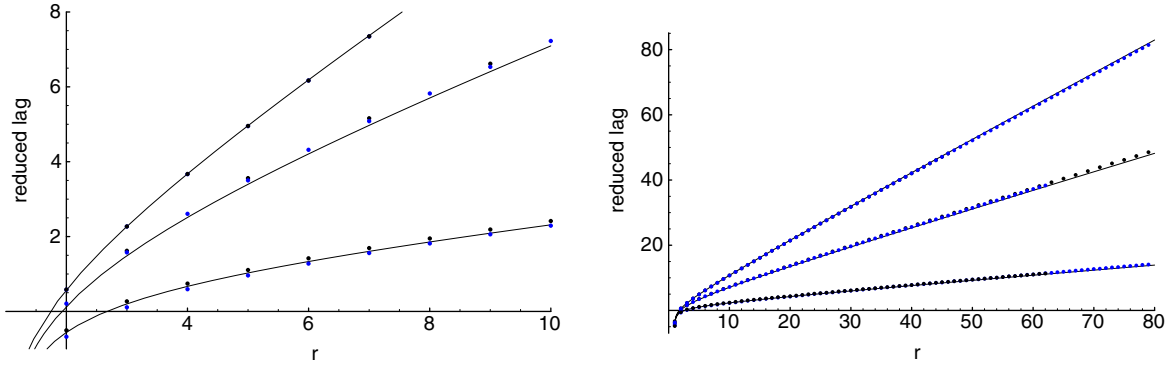

Fig. 1. Barrier-independent part of the time lag, $\tilde{t}_{\mathrm{L}}$. Eq. (38) as a function of $r = R/R_*$ for different values of the 'discreteness parameter' $a \equiv 2W_*/Tn_*$ on an intermediate (left figure) and large (right figure) scales, respectively. In each of the figures the upper line represents the Zeldovich–Frenkel limit, Eq. (14) for $a \to 0$. The two other lines are from general asymptotic Eqs. (13) and (19) with $a = 4$ (middle line) and $a = 8$ (lower line) respectively. Symbols are from Eq. (38) using exact results for $t_{\mathrm{L}}^{\mathrm{c}}$ for $a = 0.4$ (which is indistinguishable from the ZF limit), $a = 4$ and $a = 8$. The reduced barriers W_*/T were chosen as 20 and 40 ($a = 0.4$), 40 and 80 ($a = 4$), 80 and 160 ($a = 8$): in each case n_* was selected to provide the indicated a.

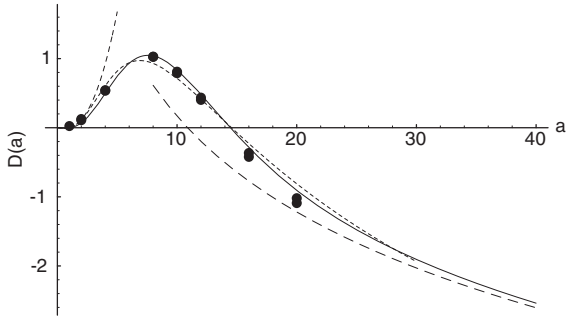

Fig. 2. The barrier- and size-independent part of the incubation time, $D(a)$ in Eq. (39). Solid lines – from Eq. (25), symbols – from exact time-lag. (In the latter case two different pair of values for the barrier W_*/T and the critical number n_* were considered at each value of a, with resulting minor scatter at large a.) Dashed lines are corresponding asymptotes at small a, Eq. (34) and large a. Eq. (32), respectively. The interpolating dotted line is Eq. (36).

The dependence of $D(a)$ is rather sophisticated, being negative at very small a. then passing through a shallow minimum near $a \approx 0.6$, and changing sign near $a \approx 1$. A maximum $D(a) \approx 1$. is achieved near $a \approx 7.6$. Approximately, one could write

$$D(a) \approx 1 + \delta a/34 - (\delta a/4.4)^2 - (\delta a/6)^3, \quad \delta a \simeq a - 7.6, \tag{40}$$

which is valid for $1 \lesssim a \lesssim 10$, and covers the domain of practical interest [10,11]. However in the quest for simplicity and due to relative smallness of D (and the opposite, often comparable contribution of the lower boundary), in some applications it can be reasonable to neglect its value.

For $a\zeta(r) \ll 2\pi$, accuracy of describing the size-dependence can be systematically improved by including into Eq. (39) higher-order corrections, as in Eq. (29). In practice, validity of the approximation is manifested by the relatively small values of the corrections to the starting ZF expression, and by the diminishing contribution of terms with higher powers of a. Most of numerical studies, typically carried out for $r \lesssim 2$, e.g. the one by Kelton et al. [10], are expected to be within this domain. The study of Granasy and Games [11] at larger r, with $a\zeta \lesssim 3.5$, could require a few extra terms in the expansion, but the main approximation (39) works here reasonably accurately, as will be discussed below, and within the reported scale of data in Ref. [11] it could be hard to look for further improvements.

3.3. The effect of lower boundary

As mentioned, placing the lower boundary at a finite $r_{\min}$ reduces $t_i(r)$ by an r-independent constant, determined by the 'decay time', $t_{\rm dec}(r_{\min})$. This modifies the constant in Eq. (39):

$$D(a) \to D(a) - t_{\rm dec}(r_{\min}). \tag{41}$$

Using Eqs. (19) and (A.5) one has

$$t_{\rm dec}(r_{\min}) \simeq -\sum_{n=1}^{n_{\min}} 1/\dot{n}. \tag{42}$$

Eq. (42) is valid for any $r_{\min}$ in the decay region (unless $r_{\min}$ is directly placed into the near-critical domain with $1 - r_{\min} \lesssim \epsilon$, which does not make much sense). In the ZF case the discrete sum should be replaced by an integral with a zero lower limit, leading to Eq. (16).

We recommend to use Eq. (42) for practical estimations, since evaluation of the sum is straightforward and typically involves less than ten terms. In order to get some analytical insight, one should distinguish between a 'low' and an 'elevated' boundary, depending on the value of $-a\zeta(r_{\min})$.

For a large $-a\zeta(r_{\min})$, the boundary is 'low', and even if a finite $r_{\min}$ is considered, the effect of such a boundary in the discrete models will be insignificant and much smaller than in the ZF case. More accurately, the lower bound of the estimation for the decay time is given by the last term in Eq. (42), i.e.

$$t_{\rm dec}(r_{\min}) \gtrsim -1/\dot{n}_{\min}. \tag{43}$$

For an upper bound, one can multiply the estimation by $1/(1 - \exp(-a/6n_{\min}))$.

In the opposite limit of small $-a\zeta(r_{\min})$ (more precisely, $-a\zeta(r_{\min}) \ll 2\pi$), one has an 'elevated' boundary. Since $r_{\min}$ is proportional to the *cubic* root of $n_{\min}$, the boundary can be 'elevated' already for rather modest values of the latter. One can check that even for $n_{\min} = 2$ most of the simulation studies [10,11] (typical $a \lesssim 4$) fall into that domain, and larger $n_{\min}$, with still smaller $-a\zeta(r_{\min})$, are often considered. The difference from the ZF model with non-negligible lower boundary, Eqs. (14)–(16), is minor. The first correction is given by

$$\delta t_i^{(1)}(a, r, r_{\min}) \simeq (F(a) - 1)(r + r_{\min} - 2) + (G(a) - 1)\ln(r r_{\min}), \tag{44}$$

with $r > 1$ and $a/2\pi \lesssim r_{\min} < 1$. Note that the coefficients $F(a) - 1$ and $G(a) - 1$ equal, respectively, $\mp a^2/24$ for small a. The next correction

$$\delta t_i^{(2)} \simeq \left(\frac{a}{5.36}\right)^4 \left[5 - 3\left(\frac{1}{r} + \frac{1}{r_{\min}}\right) + \frac{1}{2}\left(\frac{1}{r^2} + \frac{1}{r_{\min}^2}\right)\right] \tag{45}$$

is expected to be small within the domain of applicability, but can be useful in order to check the accuracy. Note the dominant contribution of $r_{\min}$ compared to r. Higher order corrections in a can be systematically obtained from the expansion in Bernoulli numbers, as in Eqs. (21) and (29), with δt_i in Eq. (20) given by $\delta t_i = \delta t_i^{(1)} + \delta t_i^{(2)} + \cdots$.

The above Eq. (44) is the second main analytical result of this paper. It can be used as an alternative to

Eq. (39) when the boundary is elevated and the reduced size r in the growth region is not necessarily large.

3.4. Transient nucleation curves

Once the incubation time is accurately predicted, one expects that the entire transient behavior also will be reproduced. Figs. 3 and 4 compare, respectively, the transient flux, Eq. (12) and the number of nuclei, Eq. (18). with results by Granasy and Jarnes [11] for rather strong discreteness effects, $a \approx 3.5$. The correspondence is good within the reported limits of accuracy. Note, that not only large, but also intermediate values of $r = 2$ and $r = 5$ are well described by Eq. (39). The effects of lower boundary were neglected, but this was partly compensated by the neglect of the constant $D(a)$ in Eq. (39) and would be bearly noticeable in the scale of Figs. 3 and 4.

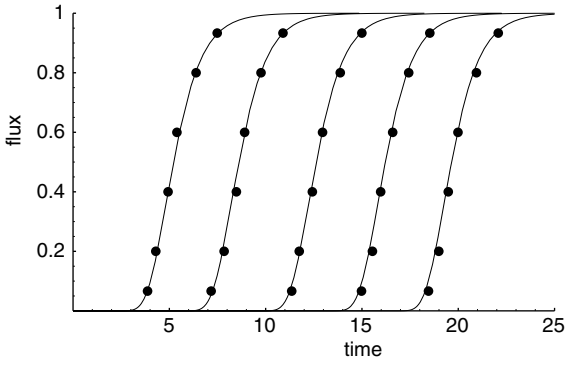

Fig. 3. The reduced nucleation flux, $j(r,t)/j_s$ as function of reduced 'time', t/τ, for different values of reduced 'radius' $r = R/R_*$. From left to right: $r = 2$, 5, 10, 15 and 20. Symbols – numerical results by Granasy and James [11]. Lines – Eqs. (12) and (39). No matching parameters were used.

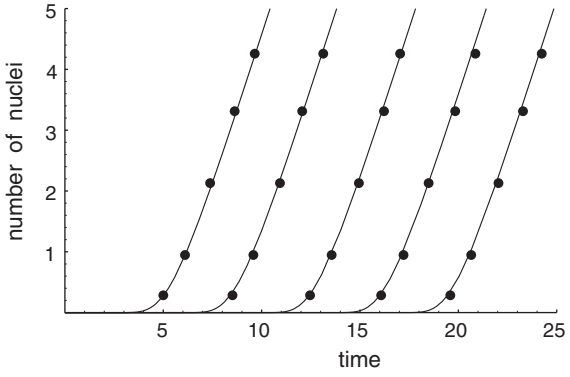

Fig. 4. Reduced numbers of nuclei $\rho(r,t)/j_s$ for different r. Comparison of Eqs. (18) and (39) with data by Granasy and James. Parameters and order of curves same as in Fig. 3.

In the numerical studies of Kelton et al. [10]. the lower boundary was placed, approximately at $n_*/2$ (i.e., $r_{\min} \sim 0.8$), and in the growth region the transient flux was reported at $n = 2n_*$ and $n = 3n_*$. The values of a were close to 4. Kelton's results should be accurately reproduced by Eq. (12) for the transient shape, together with Eqs. (14)–(16), (20), and (44) for the incubation time which take into account the lower boundary effects (although we did not perform the actual comparison). The leading TF correction, Eq. (44) in this case is small. Also, when fitting transient data of Ref. [10], Wu [26] suggested to use a log-normal curve, rather than a double-exponential given by Eq. (12). It turned out, however, that for the parameters of interest the log-normal shape and the one of Eq. (12) are virtually indistingishable [27], for which reason one can interpret Wu's comparison in support of the latter.

4. Discussion

In the present work we demonstrated the possibility of numerically exact evaluation of the time lag of transient nucleation at very large cluster sizes, up to 10^8 monomers. This significantly expands the domain of sizes typically considered in direct numerical solutions of the nucleation equations, and can serve as an accurate test for those methods. Applications of the results to analysis of experimental data also can be anticipated since the latter, especially in case of one step annealing, often characterize the transient behavior only by the time lag.

Generally, the exact expression depends on several independent dimensionless parameters, such as the reduced barrier W_*/T, number of monomers in a cluster n, critical number n_*, etc. Those dependences are nontrivial (cannot be scaled out), which can complicate the analysis of experimental data. Nevertheless, asymptotically such dependences do separate from each other. The simplest case, in which the Turnbull–Fisher and the Zeldowich–Frenkel models are equivalent to each other, corresponds to $n_* \gtrsim W_*/T \gg 1$. Here the time lag depends only on $\ln(W_*/T)$ and on an elementary function of the reduced radius $r = (n/n_*)^{1/3}$, as in Eqs. (14), (19). For smaller n_* the logarithmic dependence on the barrier still can be separated, but the remaining function of r and $a = 2W_*/Tn_*$ is non-elementary. Depending on the desired level of accuracy, or on the domain of sizes of interest, simple approximation which separate the r- and a-dependences can be constructed. The main result here is Eq. (39). which with $D \approx 0$ should be sufficient in experimental context. When comparing with exact numerics one might add the more accurate values of the constant D discussed above, and further subtract the contribution of the lower boundary. In the latter case the main result is Eq. (44) if the lower boundary is

'elevated'. Systematic expansions for small and arbitrary a are also discussed. Exact results can be used to monitor the approximations at all levels.

Connection with the full transient nucleation problem is given via Eq. (19), which relates the time lag to the 'incubation time' t_i, and via Eq. (12) which describes the transient shape or Eq. (18) which describes the number of nuclei. Good correspondence with available numerical data, as in Figs. 3 and 4 is observed.

Appendix A. Exact results for the nucleation equation

With selected boundary conditions the exact steady-state flux of Eq. (1) is given by

$$j_s^e = 1 \Big/ \sum_{n=n_{\min}}^{\infty} (1/\beta_n f_n^{eq}). \tag{A.1}$$

The infinite summation limit is formal since the sum rapidly converges beyond the critical size (and a finite upper limit originally discussed by Farkas [20] will lead to virtually identical results).

In the transient case one can get exactly the time lag. Several forms of the exact expression are available in literature [12,21,28,29] but not all are suited for the study of the region $r \gg 1$, e.g. due to the presence of exponentially growing terms. We use the form [12] slightly modified to include arbitrary lower boundary at $n = n_{\min}$. Introducing for simplicity of notations.

$$c(m,n) = \beta_m^{-1} \exp\{[W(m) - W(n)]/T\},$$

and distinguishing the exact time-lag by a superscript 'e', one has

$$t_L^e(n) = \sum_{m=n_{\min}}^{n-1} \Psi_m - j_s \sum_{m=n_{\min}}^{\infty} \Psi_m^2 \exp\{W(m)/T\} \tag{A.2}$$

with

$$\Psi_n = \sum_{m=n_{\min}}^{n-1} c(m,n), \tag{A.3}$$

for $n \leqslant n_*$ and

$$\Psi_n = \sum_{m=n}^{\infty} c(m,n), \tag{A.4}$$

for $n > n_*$, respectively. Link with the asymptotic treatment is established via a relation

$$\Psi_n \simeq \frac{1}{|\dot{n}|}, \quad |n - n_*| \gg \epsilon n_*. \tag{A.5}$$

This allows one [12] to recover the asymptotic Eqs. (13) and (19).

Appendix B. A systematic expansion of the incubation time at arbitrary a

Consider a series representation of the inverse growth rate

$$\frac{1}{\tau v(r)} = \frac{1}{\zeta(r)} + 2b^2\zeta(r) \sum_{k=1}^{\infty} \frac{(-1)^k k^{-2}}{1 + [b\zeta(r)/k]^2}, \quad b \equiv \frac{a}{2\pi} \tag{B.1}$$

with the first term corresponding to the ZF approximation. Using term-by-term integration, one obtains the correction for the incubation time

$$\frac{1}{2\tau}\delta t_i(a,r) = \sum_{k=1}^{\infty} (-1)^k \mathscr{F}\left[\frac{b}{k}, \zeta(r)\right] + \sum_{k=1}^{\infty} (-1)^k \mathscr{F}\left[\frac{b}{k}, \zeta(r_{\min})\right], \tag{B.2}$$

where the function $\mathscr{F}[b,\zeta]$ is defined in Eq. (35). Since the terms have alternating signs, a good convergence is expected.

References

[1] D. Turnbull, J.C. Fisher, J. Chern. Phys. 17 (1949) 71.
[2] P. James, Phys. Chem. Glasses 15 (1974) 95.
[3] V.M. Fokin, A.M. Kalinina, V.N. Filipovich, Fiz. Khini. Stekla 6 (1980) 148.
[4] J. Deubener, J. Non-Cryst. Solids 274 (2000) 195.
[5] E.D. Zanotto, P.P. James, J. Non-Cryst. Solids 74 (1985) 373.
[6] J. Deubener, R. Brükner, M. Sternizke, J. Non-Cryst. Solids 163 (1993) 1.
[7] S. Privitera, F. La Via, C. Spinella, S. Quilici, A. Borghesi, F. Meinardi, M.G. Grimaldi, E. Rimini, J. Appl. Phys. 88 (2000) 7013.
[8] C. Spinella, S. Lombardo, F. Priolo, J. Appl. Phys. Rev. 84 (1998) 5383.
[9] G. Nicotra, S. Lombardo, C. Spinella, G. Ammendola, C. Gerardi, C. Demuro, Appl. Surf. Sci. 205 (2003) 304.
[10] K.F. Kelton, A.L. Greer, C.V. Thompson, J. Chem. Phys. 79 (1983) 6261.
[11] L. Granasy, P. James, J. Chem. Phys. 113 (2000) 9810.
[12] V.A. Shneidman, M.C. Weinberg, J. Chem. Phys. 97 (1992) 3629.
[13] V.A. Shneidman, Sov. Phys. Tech. Phys. 32 (1987) 76.
[14] V.A. Shneidman, Sov. Phys. Tech. Phys. 33 (1988) 1338.
[15] K.F. Kelton, A.L. Greer, J. Non-Cryst. Solids 79 (1986) 295.
[16] V.A. Shneidman, M.C. Weinberg, J. Chem. Phys. 95 (1991) 9148.
[17] V.A. Shneidman, M.C. Weinberg, J. Chem. Phys. 97 (1992) 3621.
[18] V.A. Shneidman, M.C. Weinberg, MRS Symp. Proc. 398 (1996) 99.
[19] Ya.B. Zeldovich, Acta Physicochim. (USSR) 18 (1943) 1.
[20] L. Farkas, Z. Phys. Chem. 25 (1927) 236.
[21] B. Shizgal, J.C. Barrett, J. Chem. Phys. 91 (1989) 6505.
[22] M. Abramowitz, I. Stegun, Handbook of Mathematical Functions, Dover, New York, 1972.
[23] C. Rüssel, R. Keding, J. Non-Cryst. Solids 328 (2003) 174.
[24] V.A. Shneidman, D.R. Uhlmann, J. Chem. Phys. 108 (1998) 1094.
[25] V.A. Shneidman, M.C. Weinberg, J. Non-Cryst. Solids 160 (1993) 89.

[26] D.T. Wu, Nucleation theory, in: H. Ehrenreich, F. Spaepen (Eds.), Solid State Physics: Advances in Research and Applications, Academic, San Diego, 1996, p. 37.
[27] V.A. Shneidman, J. Chem. Phys. 119 (2003) 12487.
[28] (a) R. Andreas, M. Boudart, J. Chem. Phys. 42 (1965) 2057; (b) H.L. Frisch, C. Carlier, J. Chem. Phys. 54 (1971) 4326; (c) G. Wilemski, J. Chem. Phys. 62 (1975) 3772.
[29] D.T. Wu, J. Chem. Phys. 97 (1992) 1922.